Journal of Chromatography A, 1218 (2011) 1954–1965

Contents lists available at ScienceDirect

Journal of Chromatography A

journal homepage: www.elsevier.com/locate/chroma

Influence of the solvation process on solute adsorption in reversed phase liquid chromatography

Péter Vajda[a], Szymon Bocian[b], Bogusław Buszewski[b], Attila Felinger[a,*]

[a] Department of Analytical and Environmental Chemistry, University of Pécs, Ifjúság útja 6, H-7624 Pécs, Hungary
[b] Department of Environmental Chemistry and Bioanalytics, Faculty of Chemistry, Nicolaus Copernicus University, Gagarin 7, PL-87-100 Torun, Poland

ARTICLE INFO

Article history:
Available online 3 November 2010

Keywords:
Frontal analysis
Solvent adsorption
Organic modifier
Phenol

ABSTRACT

The adsorption isotherms of phenol were acquired by frontal analysis on six different reversed phase adsorbents from five different organic solvent solutions. The end-capped octadecyl columns only differed in the bonding density of the C_{18} ligands. The inverse method was used to confirm the estimated isotherm parameters derived from the frontal experiments. The effect of the bonding density of the end-capped octadecyl bonded phase on the adsorption properties of phenol from different mobile phase compositions was investigated. The adsorption behavior of phenol has changed from Langmuir type to BET type with the change of the organic modifier and the bonding density of the adsorbent.

1. Introduction

The rapid development of the applications of preparative liquid chromatography especially in the pharmaceutical industry has led to the increase of the interest in the fundamentals of nonlinear chromatography [1,2]. As a consequence, rather accurate isotherm measurement methods have been introduced and those measurements provide excellent tools to study the adsorption mechanism of solutes in liquid chromatography [3].

Silica-based alkyl bonded phases are the most popular stationary phases in reversed-phase high performance liquid chromatography (RP HPLC). The silica surface is subject to physical and chemical modification [4]. The most important advantages of those packing materials are the chemical stability and porous structure which assures rapid mass transfer, good loadability, and high reproducibility [5]. Despite the modification, the surface of reversed-phase stationary phases became heterogeneous.

In reversed-phase systems, the mobile phase is in contact with the hydrophobic surface of the stationary bonded phase. The solvents used as mobile phase adsorb on the stationary phase forming a diffuse layer on the surface. The composition of the solvents on the stationary phase depends on the thermodynamic equilibrium between both phases and it usually differs from that in the mobile phase [6]. The thickness of the stationary phase changes with mobile phase composition because of the conformation of organic ligands which are different in water and organic environment due to the solvation effects [7].

The acting stationary phase is a combination of three components: bonded ligands, residual silanols and solvent molecules adsorbed on the surface or solvated ligands [8,9]. The amount and type of the adsorbed molecules of organic solvent on the stationary phase have a strong influence on the column selectivity and the retention of the solute [10,11].

A recent study demonstrated that the adsorption behavior of the solute on the same RPLC bonded phase differs significantly whether methanol, acetonitrile, isopropyl alcohol or tetrahydrofuran was used as the organic modifier [12]. Acetonitrile, isopropyl alcohol and tetrahydrofuran are definitely more strongly adsorbed than methanol and they may compete with the compound for adsorption on the surface of the stationary phase [13,14]. This explains partly why the elution times are systematically reduced when methanol is chosen as the organic modifier. The adsorption of isopropyl alcohol is also higher than that of methanol whereas THF exhibits the highest adsorption on the octadecyl bonded phases [15].

The competition between solvent molecules and phenol is indicated on the breakthrough curves under nonlinear conditions by sub-plateaus. The stronger the eluent more pronounced the sub-plateaus emerge. This phenomena may suggest the use of competitive adsorption isotherms to describe the adsorption processes of phenol in the presence of strong eluents. On the other hand there is no change in the retention volumes of the sub-plateaus. That indicates that the surface concentration of the solvent molecules is nearly constant – the surface is saturated – at each isocratic step of the frontal analysis. The huge difference in the retention factors of the solvent molecules and phenol measured from pure water also throttle the application of competitive adsorption isotherms on such systems [12].

* Corresponding author. Tel.: +36 72 501500x4582; fax: +36 72 501518.
E-mail address: felinger@ttk.pte.hu (A. Felinger).

0021-9673/$ – see front matter © 2010 Elsevier B.V. All rights reserved.
doi:10.1016/j.chroma.2010.10.108

The goal of our work was to determine the effect of the nature of the organic modifier in the mobile phase and the coverage density of the bonded ligands on the adsorption. Adsorption isotherms of phenol were measured on the series of home-made well defined C_{18} bonded phases. Adsorption data were obtained using frontal analysis. Overloaded elution band profiles were also modeled using the equilibrium-dispersive (ED) model of chromatography.

2. Theory

2.1. Frontal analysis for isotherm determination

Frontal analysis (FA) is the most widely used and the most accurate method to characterize the adsorption processes on chromatographic adsorbents. It consists of successive replacement of the stream of mobile phase percolating through the column with streams of solutions of the studied compound of increasing, known concentration [2,16].

In order to acquire a sufficient number of data points and to achieve measurements of a satisfactory accuracy, the retention factor (k') should be between 1 and 5, thus the mobile phase composition for single-component FA measurements must be chosen accordingly [17].

Consecutive or single breakthrough curves can be recorded in a given concentration range of the analyte, and the retention times of the fronts are recorded. The adsorbed concentration of the analyte q in g/dm^3 at a given equilibrium mobile phase concentration C in g/dm^3 of solution – in the case of consecutive breakthrough curves – can be calculated as follows [18]:

$$q_{i+1} = q_i + \frac{(C_{i+1} - C_i)(V_{F,i+1} - V_0)}{V_n} \quad (1)$$

where q_i and q_{i+1} are the adsorbed concentrations of the analyte when the stationary phase is in equilibrium with the solute mobile phase concentrations C_i and C_{i+1} at the ith and $(i+1)$th step, respectively. $V_{F,i+1}$ is the inflection point of the breakthrough curve at the $(i+1)$th step, V_0 is the void volume of the system, and V_n is the volume of normalization – the volume assigned as the adsorbent. This volume is usually the volume of the stationary phase V_{sp} [18,19], an other option is to choose the volume of the bonded phase V_{bp} as V_n. In our study both normalizations were done and the results were compared.

2.2. Models of isotherms

The Langmuir model is the most commonly used isotherm equation to describe nonlinear surface processes. The model describes ideal adsorption on a homogeneous adsorption surface, and is given as [20]:

$$q = \frac{aC}{1 + b_{s1}C} = \frac{q_{s1}b_{s1}C}{1 + b_{s1}C} \quad (2)$$

where a is the initial slope of the isotherm curve, q_{s1} is the saturation capacity of the adsorbent and b_{s1} is the related equilibrium constant or distribution coefficient.

The combination of two Langmuir terms results an other isotherm that describes ideal adsorption on heterogeneous surfaces, but with the discrimination of two independent adsorption sites. The bi-Langmuir equation can be written as:

$$q = \frac{q_{s1}b_{s1}C}{1 + b_{s1}C} + \frac{q_{s2}b_{s2}C}{1 + b_{s2}C} \quad (3)$$

where q_{s1} and q_{s2} are the saturation capacities of the two independent adsorption sites, with the respective equilibrium constants b_{s1} and b_{s1}.

Brunauer et al. [21] introduced the isotherm that describes non-ideal adsorption on homogeneous adsorption surfaces. The equation for the BET isotherm is:

$$q = \frac{q_{s1}b_sC}{(1 - b_LC)(1 - b_LC + b_sC)} \quad (4)$$

where q_{s1} is the adsorbent mono-layer saturation capacity, b_s is the corresponding equilibrium constant, and b_L is the equilibrium constant of the solute–solute interactions. The higher value of b_{Lt} means a stronger tendency of the analyte to form multilayer above the adsorbent surface. When b_L is equal to zero, Eq. (4) reduces to a simple Langmuir equation.

2.3. Equilibrium dispersive model of chromatography

If the mass transfer kinetics is fast and the probe molecules have small molar weight, the mass balance of the chromatographic system can be modeled with the equilibrium-dispersive model [1]. The model for a single component is written as:

$$\frac{\partial C_i}{\partial t} + F\frac{\partial q_i}{\partial t} + u\frac{\partial C_i}{\partial z} = D_{a,i}\frac{\partial^2 C_i}{\partial z^2} \quad (5)$$

where C_i and q_i are the equilibrium concentrations of component i in the mobile and stationary phase, respectively; z the column length, t is the time, and F is the phase ratio, given as follows:

$$F = \frac{1 - \varepsilon_T}{\varepsilon_T} = \frac{1 - V_m/V_G}{V_m/V_G} \quad (6)$$

where ε_T is the total porosity, V_m is the column void volume, given as the sum of the interstitial volume and the pore volume $V_m = V_{ex} + V_{pore}$. V_G is the geometrical volume of the stainless steel tubes where the adsorbent was loaded. $D_{a,i}$ is the apparent dispersion coefficient accounts for the band broadening effects and it is given by:

$$D_{a,i} = \frac{Hu}{2} \quad (7)$$

where H is the column height equivalent to a theoretical plate. The isotherm equations give the connection between the concentration of the solute in the mobile C and stationary phases q. The isotherm model and the related isotherm parameters derived from the frontal analysis were used as initial parameters, and the mass-balance equation was solved using the Rouchon algorithm. Measured and calculated band profiles were compared by evaluating the following objective function:

$$\min \sum_i (C_i^{calc} - C_i^{meas})^2 \quad (8)$$

where C_i^{calc} and C_i^{meas} are the calculated and measured concentrations at point i, respectively. At the end of each iterative loop, the isotherm parameters are changed to minimize the objective function using a super-modified simplex algorithm [22].

3. Experimental

3.1. Materials and solvents

All stationary phases were in-house prepared on the basis of the same Kromasil 100 porous silica support with 5 μm average particle diameter (Akzo Nobel, Bohus, Sweden). The main physicochemical properties of the silica can be find elswhere [23]. For the chemical modification of the silica surface, n-dimethyl-octadecylchlorosilane (Wacker GmbH, Munchen, Germany) was used in six different concentrations to achieve six column packings with different surface coverage of the C_{18} ligands. The end capping was made using trimethylchlorosilane. All solvents (methanol,

acetonitrile, isopropyl alcohol and tetrahydrofuran) were HPLC isocratic grade, purchased from Sigma–Aldrich (Steinheim, Germany). Water was purified using Milli-Q system (Millipore, El Paso, TX, USA). All eluents were degassed in ultrasonic bath before use. The polystyrene standards used in the ISEC measurements were purchased from Polymer Laboratories (Darmstadt, Germany). Phenol was purchased from Sigma–Aldrich (Steinheim, Germany).

The phases under study were packed into 125 mm × 4.6 mm stainless steel tubes. All columns were packed using a DT 122 packing pump (Haskel, Burbank, CA, USA) under the pressure of 40 MPa. Technical details of the procedure are described elsewhere [24,25].

Six different end-capped batches were tested – each one with a different coverage density of octadecyl ligands. The surface coverage $\alpha_{C_{18}}$ changed from 0.00 μmol/m^2 up to 3.27 μmol/m^2. The column characteristics were determined using inverse size-exclusion chromatography (ISEC) measurements.

3.2. Apparatus

The degree of coverage of the surface by alkylsilyl ligands (α_{RP}) was calculated on the basis of the elemental analysis determined with a Model 240 CHN analyzer (Perkin Elmer, Norwalk, USA).

The adsorption isotherm measurements were all carried out using an Agilent (Palo Alto, CA, USA) 1100 liquid chromatograph. The instrument includes a binary-solvent delivery system, an autosampler with a 100 μL sample loop, a diode-array UV detector, a column thermostat and a data station. The column thermostat was used to obtain a constant temperature of 298 K.

4. Results and discussion

4.1. Inverse size-exclusion chromatography

The characterization of the column physical properties is crucial in the investigation of adsorption processes. Even a relatively small deviation from the real hold-up volume of the column can lead to a complete misunderstanding of the adsorption processes [26].

Inverse size exclusion chromatography can give a detailed view of column properties, and is a very useful tool for the characterization of adsorbent surfaces. The stochastic theory of size-exclusion chromatography was used to determine the critical column properties from the experimental data.

The volume of the mobile phase V_m and the interstitial volume V_{ex} of the columns were measured using mono-disperse polystyrene standards of molecular weights of M_W = 580, 1480, 3070, 3950, 5120, 6930, 10,100, 31,420, 70,950, 170,800, 578,500, 1,233,000, and 325,000 Da, respectively. The polystyrene standards with molecular weight of higher than 70,950 Da were entirely excluded from the adsorbent pores. For the column void volume and pore volume measurements, polystyrene standards with molecular weight between 580 and 6930 Da were used. The polystyrene standards were dissolved in HPLC-grade tetrahydrofuran, which was also used as a mobile phase in the ISEC measurements.

The calculation of the radius of gyration of the polystyrene molecules is essential to estimate the size of each polystyrene molecule in the liquid phase. To convert molecular weight M_W [g/mol] to gyration radius r_G [nm] the following equation was used [27]:

$$r_G = \frac{k_B T M_W^B}{4\pi\eta K} \tag{9}$$

where k_B is the Boltzmann constant, T is temperature [K], B is equal to 0.549, η is the carrier viscosity [N m^2/s] and K is equal to 3.0×10^{-8} [m^2/s]. The retention volumes of the polystyrene standards were corrected with the extra column contributions, and the corrected retention volumes V_R were plotted against the radius of gyration of the polystyrene standards, and nonlinear fit was performed to estimate the column properties using the following equations [27]:

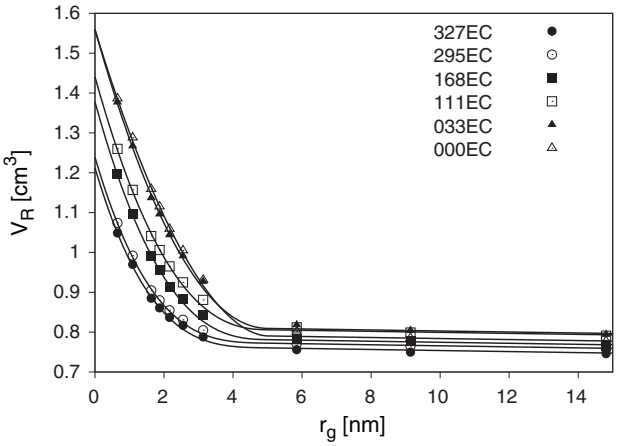

Fig. 1. The retention volumes of the polystyrene standards versus the radius of the gyrations, and the best fitted stochastic model. The column codes refers to Table 1.

$$V_R = \frac{V_{ex}}{1 + 2\lambda - C\lambda^2} + V_{pore}\left(1 - \frac{r_G}{r_p}\right)^m \tag{10}$$

and

$$V_R = \frac{V_{ex}}{1 + 2\lambda - C\lambda^2} \tag{11}$$

with

$$\lambda = \frac{3\sqrt{\pi}}{2}\frac{r_G}{d_{part}}\frac{1 - \varepsilon_e}{\varepsilon_e} \tag{12}$$

where C is a constant equal to 2.698, V_{pore} the pore volume of the adsorbent, r_p is the mean pore radius of the bare silica-gel, m is the total pore shape factor, V_{ex} is the interstitial volume of the column, d_{part} is the particle diameter, and ε_e is the external porosity. Eq. (10) was fitted in the case for $r_G < r_p$, and Eq. (11) for $r_G > r_p$. The estimated parameters derived from the fitting procedures are V_{ex}, V_{pore}, and m for each column.

The plots of the retention volumes of the polystyrene standards and the best fitted stochastic models are shown in Fig. 1. The retention volume of the polymer standards decreases as the radius of gyration, r_g increases. Table 2 summarizes the major properties of the six stationary phases derived from the ISEC measurements.

We assumed that the pore diameter of the lowest coverage density (000EC) column is equal the pore diameter of bare silica gel. The value of r_p = 5 nm was obtained from the vendor and confirmed by low-temperature nitrogen adsorption measurement [23]. For the lowest coverage density column, parameter m was fitted and a value of m = 1.84 was obtained. That value of m is rather close to the integer dimension of m = 2 and that indicates a cylindrical pore shape [27]. The above determined parameter m = 1.84 was used for the ISEC analysis of the other stationary phases and we assumed that the accessible pore diameter decreases as the coverage density of bonded phase increases. The change of the pore diameter against the surface coverage of the adsorbent is shown in Fig. 2.

The volume of the bonded ligands was estimated on the basis of the carbon load of the columns, and the results from the fit of the stochastic model of ISEC. The pore volumes of the six columns were plotted against the carbon load and linear regression was performed. Fig. 3 shows the result of the fit. The value of the y-intercept represents the 'ligand-free' bare silica column $V_{pore,0}$, assuming a constant mass of the silica in each column. The maximum devia-

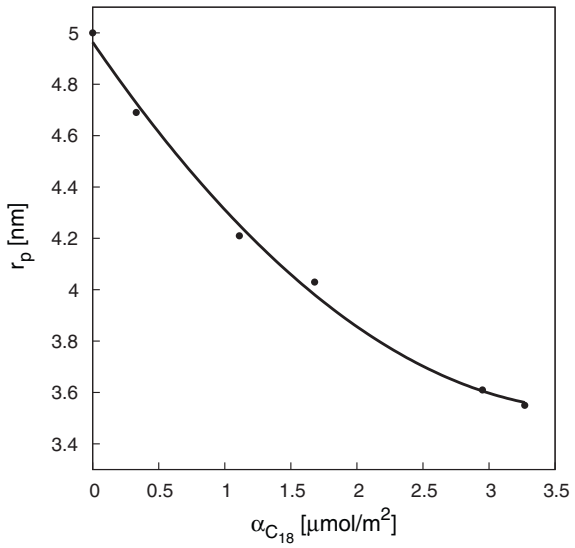

Fig. 2. Plot of the total shape factor of the pores m versus carbon load, and extrapolation to the bare silica column.

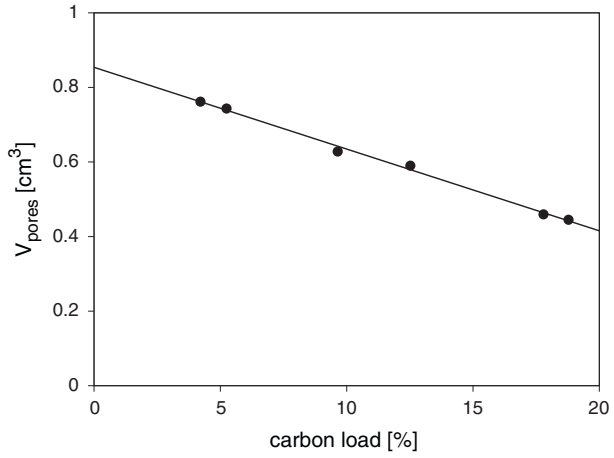

Fig. 3. Plot of the pore volumes V_{pore} of the investigated columns versus the carbon load, and the linear fit to estimate the pore volume of the theoretical column with no bonded ligands (0 carbon load), assuming same amount of silica gel each columns.

tion of the interstitial volumes V_{ex} from the average does not exceed 3.3%, which suggests that the modification of the silica gel does not significantly affect the interstitial volumes – thus the mass of the naked silica in the stainless steel tubes is constant. The $V_{pore,0}$ value becomes 0.861 cm^3. Using the specific pore volume of the silica gel 0.87 g/cm^3, one would obtain m_{silica} = 0.9891 g. The volume of the bonded ligands V_{ligand} can easily be calculated by subtracting the the pore volume of the actual column from the $V_{pore,0}$ value. The column characteristics and the results of the estimation of the volume of the bonded ligands are listed in Table 1.

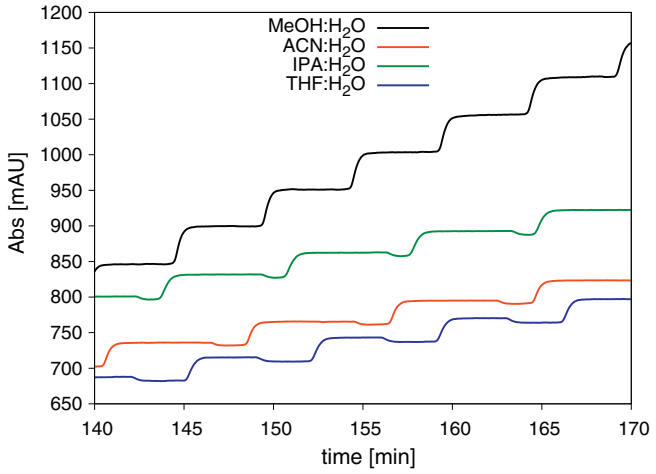

Fig. 4. Step-wise breakthrough curves of phenol on the 168EC column from the four different mobile phase compositions detected at 293 nm.

4.2. Frontal analysis of phenol

The percentage of the organic modifier in hydro-organic mixtures used as mobile phase during our experiments were 20, 30, 25 and 40 v/v% for methanol (MeOH), acetonitrile (ACN), isopropyl alcohol (IPA) and tetrahydrofuran (THF), respectively. The maximum concentrations of phenol in the mother solution were 80, 30, 35, and 10 g/dm^3 with methanol, acetonitrile, isopropyl alcohol and tetrahydrofuran as the organic modifier, respectively. The applied concentrations were chosen according to the solubility of phenol, and to achieve sufficient retention factor even on the lowest surface coverage column. Detection was carried out measuring UV absorbance at λ = 293 nm, the temperature during the measurements was constant 298 K. Consecutive breakthrough curves were recorded at a constant flow rate of 1.0 cm^3/min in all experiments.

4.2.1. Determination of adsorption isotherm data

Step-wise frontal analysis was used for every mobile phase compositions to determine the effect of the organic modifier on the adsorption properties of phenol. Pump A delivered the pure mobile phase and pump B the mother solution of phenol. Twenty-five consecutive breakthrough curves were recorded with a constant 4% increase of the concentration of the mother solution between zero and the maximum concentration of phenol at the given mobile phase composition. Fig. 4 shows the second part of the breakthrough curves of phenol dissolved in the four hydro-organic mixtures recorded on the 168EC column. The appearance of sub-plateaus was observed at higher concentrations in the order of magnitude of IPA < ACN < THF. The presence of the sub-plateaus is more expressed at low surface coverage of the octadecyl chains. No such phenomena was observed when methanol was used as organic modifier. Sub- and primary plateaus are generally observed in the case of binary frontal analysis with analytes with compa-

Table 1
Main properties of the six in-house-made RP C_{18} end-capped columns.

Column	$\alpha_{C_{18}}$ [μmol/m^2]	Carbon load [%]	V_G [cm^3]	V_{ex}[a] [cm^3]	V_{pore}[a] [cm^3]	r_p[a] [nm]	V_{bp}[b] [cm^3]	V_{sp}[a] [cm^3]
327EC	3.27	18.78	2.08	0.77	0.45	3.55	0.41	0.86
295EC	2.95	17.79	2.08	0.78	0.46	3.61	0.39	0.84
168EC	1.68	12.52	2.08	0.79	0.59	4.03	0.26	0.70
111EC	1.11	9.64	2.08	0.81	0.63	4.21	0.23	0.64
033EC	0.33	5.24	2.08	0.82	0.74	4.69	0.11	0.52
000EC	0.00	4.21	2.08	0.80	0.76	5.00	0.09	0.52

[a] Derived from the fitting procedure of the stochastic theory of ISEC.
[b] Based on own estimation.

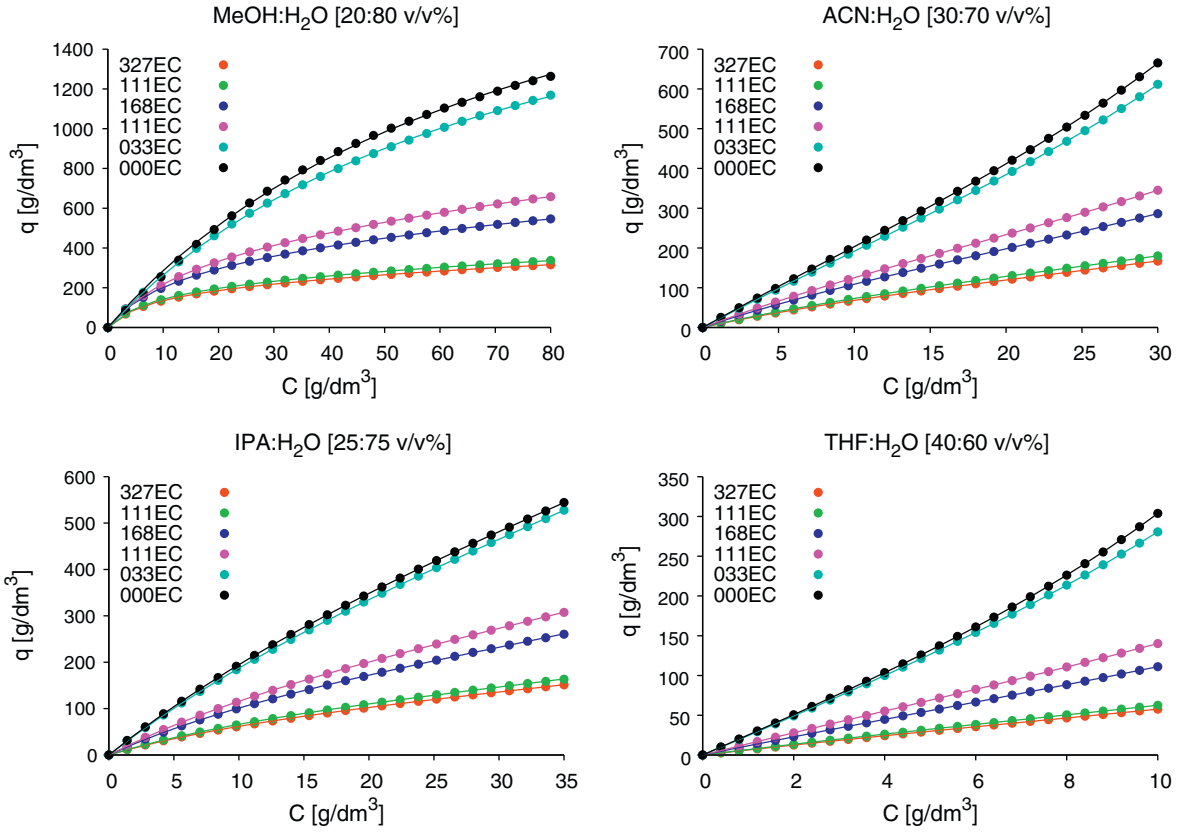

Fig. 5. Adsorption isotherm data points and the best fitted isotherm models on the six reversed phase columns.

rable retention factors [28]. Usually, the presence of sub-plateaus indicates competitive adsorption, which modifies the adsorption process, and the recorded chromatogram.

The competitive nature of the organic solvent is the function of its physico-chemical properties. It is known from excess isotherm measurements that aprotic molecules occupy a significant volume of the pores, while the pores are more water-rich in the case of alcohols as organic solvent [29]. The on-set of sub-plateaus is connected with the affinity of the solvent molecule to the hydrophobic surface. More apolar the molecule the bigger is the enrichment of the molecule at the dividing surface, which can be observed as increasing number of the formed monolayers of organic modifier above the adsorbent surface [15]. The higher affinity of the modifier results in the more effective blocking of the higher energy adsorption sites.

The decrease of the surface coverage of the C_{18} chains results in a parallel increase in the pore volume and the amount of organic modifier in the pores. This increased amount of the strong eluent in the pores results in larger competitive pressure in vying for the adsorption sites and will modify the retention time of the fronts compared to what is expected in the ideal case. In the ideal case of the single component systems, we assume the simplification that the solvent is not adsorbed, and that is more or less true in the case of methanol on columns with higher surface coverages.

4.2.2. Modeling of adsorption isotherms

The derivatives of the breakthrough curves were calculated and the inflection points corresponding to the fronts of the primary plateaus were assumed as the retention times of the fronts. Eq. (1) was used to calculate the adsorbed amount of phenol at a given mobile phase composition and concentration. The normalization volume was the volume of the stationary V_{sp}, and the volume of the bonded phase V_{bp}.

The isotherm data points were plotted and a nonlinear fit of the isotherm models was performed and the sums of squares of the residuals were compared. The isotherm model with significantly lower RSS value was chosen to describe the adsorption of phenol on the given adsorbent under the given experimental conditions.

Fig. 5 summarizes the data points and the best fitted isotherm curves. The isotherms of phenol from methanol–water mixture show Langmuir-type adsorption. On the other hand, from the stronger eluents, phenol shows BET-type multilayer adsorption behavior. The resulting parameters of the nonlinear fits are listed in Table 2.

The normalization of the isotherm data was executed by two different ways. The first and classical approach is the use of the stationary phase volume for normalization (V_{sp}). That stationary phase volume is defined as a volume what is not accessible for the mobile phase inside the geometrical volume of the column tubing. V_{sp} can divided up into two parts in the respect of the adsorption processes. The first part of the stationary phase is obviously inert for the adsorption processes, this is the volume of the silica-support. The second part of the stationary phase plays the important part in adsorption processes, this is the region of physico-chemical interactions what responsible for the separation processes. Those influences are summarized in the volume of the bonded phase (V_{bp}). This volume contains not only the bonded alkyl ligands, but also the molecules in the solvated sphere of the ligands, and the residual silanol groups. The use of different normalization volumes only affects the saturation capacity values (initial slope of the isotherm), the equilibrium constants remain intact (same curvature).

The general behavior of phenol in the presence of methanol can be handled as a starting point in the comparison of the solvent effects. The data published in the literature agree that phenol has multi-Langmuir behavior from aqueous solution of methanol. The two-site model assumes heterogeneous adsorption surface is

Table 2
Isotherm parameters determined with frontal analysis.

Column	V_n	MeOH:H_2O [20:80 v/v%]				ACN:H_2O [30:70 v/v%]		
		C_{phenol} = 80 g/dm^3				C_{phenol} = 30 g/dm^3		
		q_{s1} [g/dm^3]	b_{s1} [dm^3/g]	q_{s2} [g/dm^3]	b_{s2} [dm^3/g]	q_s [g/dm^3]	b_s [dm^3/g]	b_L [dm^3/g]
327EC	V_{sp}	93.66	0.1370	276.2	0.0037	83.47	0.0484	0.0097
	V_{bp}	198.1		584.3		176.6		
295EC	V_{sp}	98.76	0.1335	277.3	0.0041	90.24	0.0474	0.0096
	V_{bp}	210.1		589.8		192.0		
168EC	V_{sp}	119.2	0.0996	345.3	0.0051	111.5	0.0437	0.0107
	V_{bp}	316.2		915.6		295.7		
111EC	V_{sp}	147.6	0.0716	611.0	0.0027	123.8	0.0414	0.0113
	V_{bp}	416.5		1724		349.1		
033EC	V_{sp}	481.8	0.0132			123.3	0.0350	0.0133
	V_{bp}	2261				578.7		
000EC	V_{sp}	444.9	0.0129			105.6	0.0358	0.0140
	V_{bp}	2506				595.1		

Column	V_n	IPA:H_2O [25:75 v/v%]			THF:H_2O [40:60 v/v%]		
		C_{phenol} = 35 g/dm^3			C_{phenol} = 10 g/dm^3		
		q_s [g/dm^3]	b_s [dm^3/g]	b_L [dm^3/g]	q_s [g/dm^3]	b_s [dm^3/g]	b_L [dm^3/g]
327EC	V_{sp}	76.18	0.0513	0.0071	51.56	0.0592	0.0197
	V_{bp}	161.2			109.1		
295EC	V_{sp}	81.13	0.0510	0.0073	50.29	0.0658	0.0218
	V_{bp}	172.6			107.0		
168EC	V_{sp}	105.0	0.0469	0.0076	70.21	0.0629	0.0240
	V_{bp}	278.5			186.2		
111EC	V_{sp}	124.7	0.0409	.0071	76.68	0.0659	0.0269
	V_{bp}	351.9			216.3		
033EC	V_{sp}	145.9	0.0321	0.0066	78.82	0.0657	0.0342
	V_{bp}	684.7			370.0		
000EC	V_{ads}	139.7	0.0288	0.0056	54.46	0.0820	0.0412
	V_{bp}	787.3			306.8		

the one that fits best on the four columns with higher surface coverage. The surface heterogeneity has two main origin. First, the column packing is heterogeneous itself, elemental impurities, nonuniform particles and chemical modification have to be taken into account. Second, the heterogeneity of the adsorption of the probe compound, that becomes obvious during the modeling of the isotherm data. The two-site model assumes two global adsorption sites, one with higher energy located within the bonded layer (possible interactions between the phenolic-group of phenol and residual silanols), and the second somewhere near the interface between the bulk mobile- and stationary phase (apolar interactions between the phenyl-ring and the bonded ligands) [30]. With the decrease of the retention factor of phenol, the simple Langmuir model gives the best result on the two columns with the lowest surface coverage. The effect of the coverage density on the retention properties of phenol from water–methanol mixtures is discussed detailed by Gritti and Guiochon [31].

Replacing methanol with a stronger eluent as organic modifier, results in a fundamental change in the shape of the adsorption isotherms of phenol. For 2-propanol, acetonitrile, and tetrahydrofuran the BET model describes best the adsorption on every adsorption bed, regardless of surface coverage.

Fig. 6 gives a graphical overview of the change of the adsorption parameters of phenol from different mobile phases. The saturation capacity q_s of the adsorbents decreases radically when organic modifiers other than methanol are used. The biggest decrease of the saturation capacity can be observed from tetrahydrofuran–water mixtures. The solvent molecules effectively block a significant amount of the adsorption sites, which are accessible when the bonded phase is solvated with methanol–water mixture. This hamper is more extensive when the hydrophobicity of the organic modifier is stronger. Two equilibrium constant of the adsorption – b_{s1}, and b_{s2} – can be discriminated in the case of methanol–water mobile phase. The first one represents the high energy sites and describes the partition processes into the bonded phase. The second one characterizes the lower energy sites due to the adsorption processes. The equilibrium constants of the higher energy sites decrease as the surface coverage of the C_{18} ligands decreases, and below a point, the discrimination between partition and adsorption becomes impossible. The larger the distance between the bonded ligands, the energy of partition becomes lower, and on the 033EC column the energy of the partition and adsorption are close to each other, and with the elimination of the C_{18} ligands (000EC) only the adsorption processes are possible. The solvent molecules occupy the high energy sites, the equilibrium constant of the partition disappears. The solvation of the ligands causes an enrichment of the more apolar molecules in the bonded phase. That increases the apolarity of the pores, thus the energy of adsorption increases. The b_L values are zero in the case of Langmuir isotherms, and they grow with the increase of the influence of the solvent molecules on the adsorption of phenol. The apolar solvents affect more significantly the adsorption processes than the protic ones. The b_L values are good indicators for the deviation from the 'ideal' Langmuirian behavior.

With the decrease of the C_{18}-ligand density, higher water enrichment can be assumed on the unreacted silanols, with the decrease of the surface apolarity. Parallel with the increase of the water enrichment above the surface the adsorbed monolayers of the organic modifier decrease. The strongest decrease was observed in the case of aprotic solvents [15]. This suggest a more and more water-rich mixture of organic modifier above the surface. This mixture with the combination of the apolar interactions with the C_1 and C_{18} alkyl-ligands is responsible for the stronger multilayer adsorption of phenol from stronger eluents with the decrease of the surface coverage of the octadecyl-ligands.

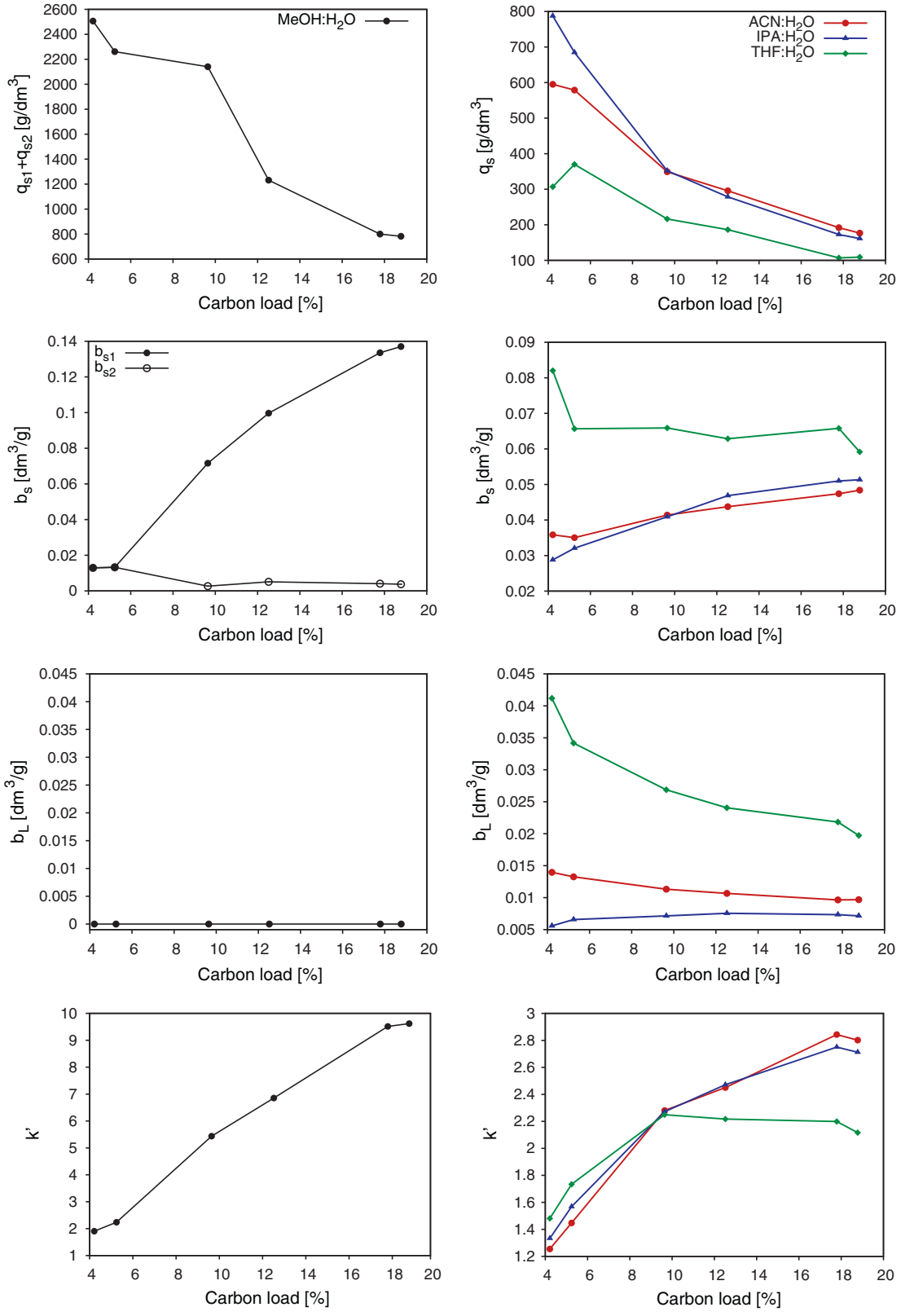

Fig. 6. Graphical representation of the change of the adsorption isotherm parameters, and the retention factor of phenol from the four different mobile phases. Note that $b_L = 0$ value results in a Langmuir isotherm.

The retention factor of an infinite diluted sample k' can be calculated using the phase ratio F and the initial slope of the isotherm constant a of the isotherm:

$$k' = Fa \tag{13}$$

If V_n was chosen as the volume of the bonded ligands, the change in the initial slope of the isotherm have to be taken into account. Eq. (6) have to be modified, the geometrical volume of the column needs correction with the volume of the silica gel in the column

V_{silica}, to get the correct value of the retention factor. The corrected geometrical volume is given by: $V_{G,corr} = V_G - V_{silica}$.

The drastic decrease in the retention factor of phenol from methanol–water changes to moderate one for the other mobile phases. The order of the retention factor of phenol from stronger eluents changes on the two columns with the lowest carbon content. Phenol gives the lowest retention factor from tetrahydrofuran–water mixture on columns with high surface coverages of the C_{18} ligands, but it becomes the highest on the two columns with lower surface coverage. The transition point is around the surface coverage of 1.68 μmol/m^2. When the surface coverage is below a threshold, the effect of the residual silanols becomes significant on the analyte retention. More apolar the organic modifier, its exclusion from the deeper segment of the bonded phase will strengthen. This will hamper the solvation processes, and the least polar tetrahydrofuran become a weaker competitor, and the decrease of the retention factor of phenol become moderate. The second highest k' decrease after methanol between high and low carbon load columns can be observed in the case of acetonitrile. Between tetrahydrofuran and acetonitrile, isopropyl-alcohol represents the midpoint, as moderate apolar protic solvent.

4.3. Modeling of overloaded elution bands of phenol

The inverse method was employed to model and fit the overloaded elution bands of phenol from the various solvent systems. The method gives an independent and fast isotherm parameter estimation. It is a tool to confirm and compare the adsorption data derived from the FA measurements. The measurements of the overloaded elution bands were performed using the same solvents and solutions as during the frontal analysis. Pump A delivered the pure mobile phase, and pump B performed the injection of the 2.0, 1.5, 1.0, and 0.5-min long pulse of phenol dissolved in the mobile phase. Then the bands were eluted with the pure mobile phase. The overloaded bands were recorded using the same wavelength and temperature as in the case of frontal analysis, with a constant flow rate of 1.0 cm^3/min.

4.3.1. The boundary conditions

The inlet profile represents the boundary condition of the mass-balance equation, so the accurate description is necessary for modeling overloaded elution bands [32]. During the inlet profile measurements, the column was replaced by a zero-volume connector to estimate the effect of the dead volume of the system on the overloaded elution bands of phenol. In the minute of injection, the concentration profile is a rectangular impulse with sharp boundaries, but when one injects the analyte into pure mobile phase a rapid dispersion takes place immediately during the migration through the connecting capillaries and the rectangular pulse will erode and broaden. This band broadening effect, or extra-column contributions can be separated into three main reasons [33]: (1) axial dispersion in the connecting tubes, (2) exponential tailing because of mixer-type effects, (3) finite width of the injection pulse. To take into consideration all those contributions, the convolution of a Gaussian curve, an exponential decay function, and a rectangular plug was used to describe the boundary conditions of the equilibrium dispersive model [34]. The resulting equation is the modified-exponentially modified gaussian (EMG) function [35]:

$$C(t) = \frac{1}{2a}\mathrm{erfc}\frac{t_0 - t}{\sqrt{2}\sigma} - \mathrm{erfc}\frac{t_p + t_0 - t}{\sqrt{2}\sigma} + \exp\left(\frac{\sigma^2}{2\tau^2} + \frac{t_0 - t}{t}\right) \times \left[e^{t_p/\tau}\mathrm{erfc}\left(\frac{\sigma}{\sqrt{2}\tau} + \frac{t_p + t_0 - t}{\sqrt{2}\sigma}\right) - \mathrm{erfc}\left(\frac{\sigma}{\sqrt{2}\tau} + \frac{t_0 - t}{\sqrt{2}\sigma}\right)\right] \quad (14)$$

where t_0 is the residence time in the connecting tube, σ the Gaussian band width (axial dispersion) and τ the time constant of the mixer-type extra column volume and t_p is the injection time of a narrow rectangular pulse.

4.3.2. Calibration

The equilibrium-dispersive model of chromatography requires chromatograms in concentration, and not in detector signal units. Before modeling of the overloaded bands, the conversion to the concentration units has to be made. In the case of methanol–water solution, the nonlinearity of the detector response needed nonlinear calibration, based on the absorption of the plateaus at a given concentration. The nonlinear calibration was done using the following polynomial equation:

$$C = p_1A + p_2A^2 + p_3A^3 + p_4A^4 \quad (15)$$

where p_1, p_2, p_3, and p_4 are the fitted parameters.

In the case of the other mobile phases the calibration processes were carried out using a method based on the peak areas of overloaded bands.

The amount of the injected sample can be derived after the integration of the elution band:

$$m_{inj} = \int C(V)dV = F_v \int C(t)dt \quad (16)$$

where $C(V)$ is the concentration, and m_{inj} the mass of the injected sample and it is given by $m_{inj} = V_{inj}\,C_{inj}$, where V_{inj} and C_{inj} are the volume and the concentration of the injected sample, respectively. F_v is the flow rate, The connection between detector signal and concentration can be derived as:

$$A(t) = kC(t) \quad (17)$$

where $A(t)$ is the detector response at the given time t, and k is a response coefficient. The response coefficient k can be derived as follows:

$$A_T = \int A(t)dt = k\int C(t)dt = \frac{km_{inj}}{F_v} \quad (18)$$

$$k = \frac{A_TF_v}{m_{inj}} \quad (19)$$

where A_T is the area of the measured peak. The absorbance signals of the overloaded elution bands were converted to concentration using Eq. (19).

4.3.3. Determination of isotherm parameters using the inverse method

The isotherm parameters were derived from the overloaded bands with highest injected amount of phenol. The isotherm models, and the initial parameters were determined from the FA experiments. The initial parameters were changed, to minimize the difference between measured and calculated overloaded bands. Fig. 7 gives an overview of the experimental and simulated elution profiles of phenol from the four eluents on three selected columns. The estimated parameters derived from the inverse method are summarized in Table 3.

The derived parameters are in good agreement with the FA measurements on high surface coverages, with weaker eluents. The deviation is the highest from the 'ideal' ED-model is in the case of tetrahydrofuran–water mixture on the 000EC (C_1) column. The ED-model contains simplifications, all the kinetic band broadening effects are lumped into one apparent diffusion term, it assumes instantaneous adsorption etc. We can model the experimental system in the case of alcohols relatively good, but in the case of the protic solvents the diffusion processes, and the 'ideal adsorption' is far from the ideal state. This effects results the moderate agreement

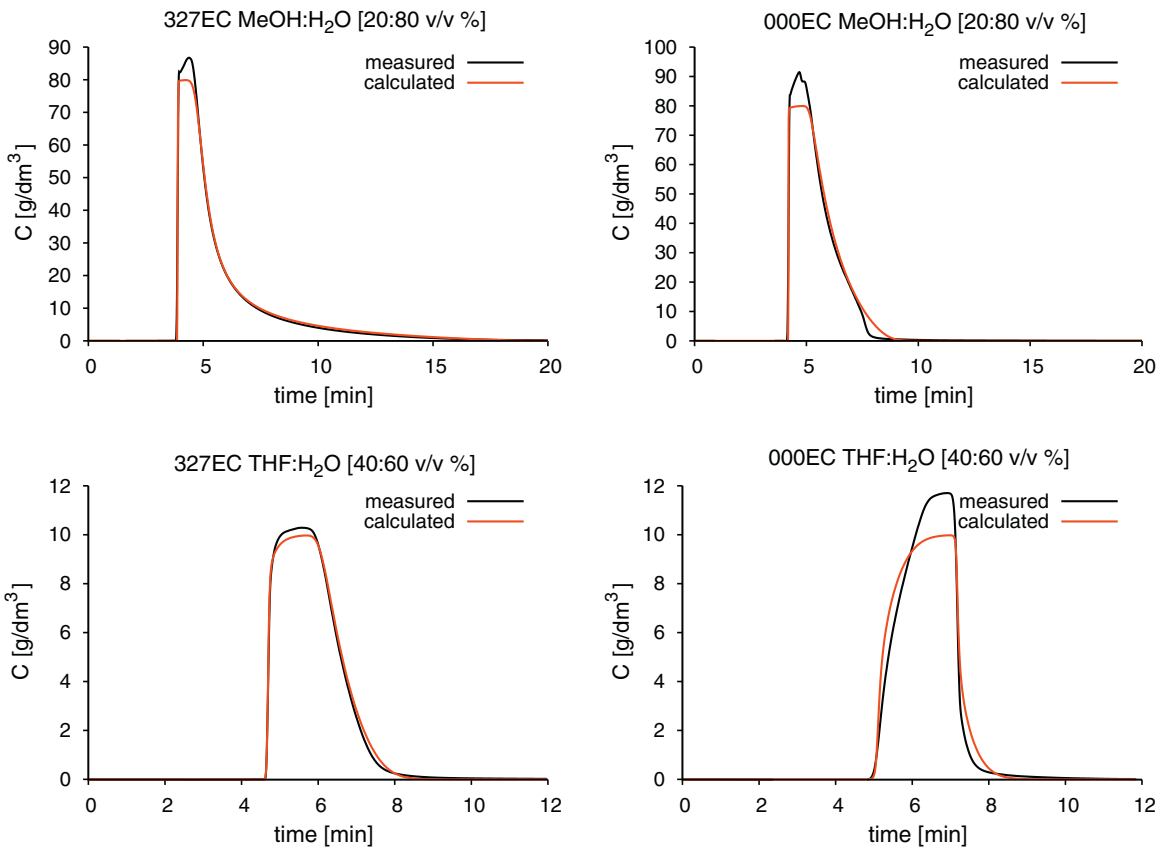

Fig. 7. Comparison of the theoretical (calculated using the inverse method), and the experimental (measured) overloaded elution bands of phenol on columns with high and low surface coverage of the C_{18} ligands. The injection volumes were uniform 2.0 cm^3.

Table 3
Isotherm parameters determined by the inverse method.

Column	V_n	MeOH:H_2O [20:80 v/v%]				ACN:H_2O [30:70 v/v%]		
		C_{phenol} = 80 g/dm^3				C_{phenol} = 30 g/dm^3		
		q_{s1} [g/dm^3]	b_{s1} [dm^3/g]	q_{s2} [g/dm^3]	b_{s2} [dm^3/g]	q_s [g/dm^3]	b_s [dm^3/g]	b_L [dm^3/g]
327EC	V_{sp}	92.87	0.1428	282.5	0.0039	88.83	0.0535	0.0092
	V_{bp}	196.5		597.7		187.9		
295EC	V_{sp}	99.70	0.1357	284.4	0.0041	98.3	0.0497	0.0089
	V_{bp}	212.1		605.0		209.1		
168EC	V_{sp}	115.0	0.1042	341.7	0.0053	121.9	0.0474	0.0100
	V_{bp}	305.1		906.3		323.4		
111EC	V_{sp}	146.0	0.0733	621.9	0.0028	137.1	0.0450	0.0102
	V_{bp}	411.9		1754		386.8		
033EC	V_{sp}	488.6	0.0132			166.8	0.0315	0.0102
	V_{bp}	2425				782.9		
000EC	V_{sp}	488.6	0.0130			170.9	0.0268	0.0097
	V_{bp}	2752				962.8		

Column	V_n	IPA:H_2O [25:75 v/v%]			THF:H_2O [40:60 v/v%]		
		C_{phenol} = 35 g/dm^3			C_{phenol} = 10 g/dm^3		
		q_s [g/dm^3]	B_s [dm^3/g]	b_L [dm^3/g]	q_s [g/dm^3]	b_s [dm^3/g]	b_L [dm^3/g]
327EC	V_{sp}	80.66	0.0553	0.0068	52.02	0.0692	0.0175
	V_{bp}	170.6			110.7		
295EC	V_{sp}	88.13	0.0542	0.0065	50.63	0.0773	0.0196
	V_{bp}	187.5			107.7		
168EC	V_{sp}	110.9	0.0535	0.0070	69.75	0.0765	0.0210
	V_{bp}	294.2			185.0		
111EC	V_{sp}	134.3	0.0444	0.0067	81.18	0.0749	0.0219
	V_{bp}	378.7			229.0		
033EC	V_{sp}	158.9	0.0338	0.0065	106.7	0.0571	0.0224
	V_{bp}	746.1			500.7		
000EC	V_{ads}	156.4	0.0299	0.0057	82.53	0.0657	0.0267
	V_{bp}	880.9			465.0		

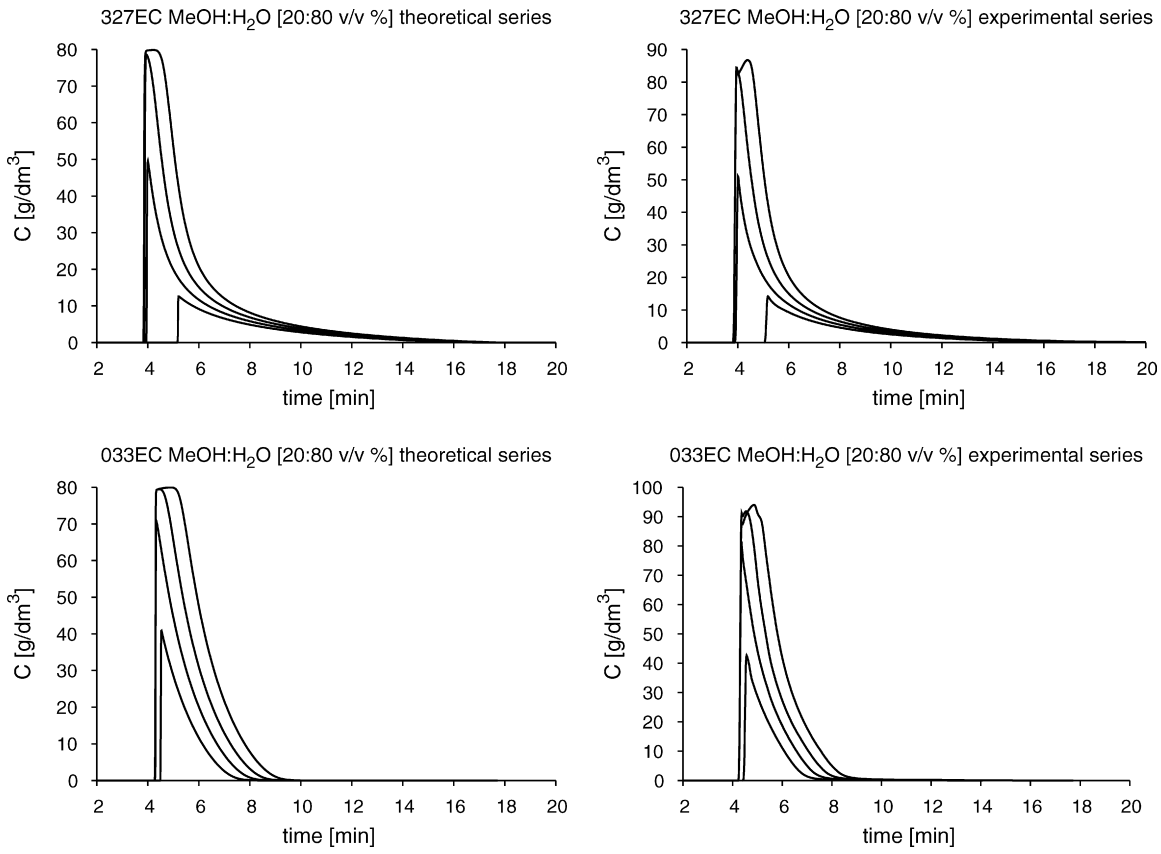

Fig. 8. Comparison of the theoretical, and the experimental series of overloaded elution bands of phenol from methanol–water mixtures on two selected columns. The injection volumes were 0.5, 1.0, 1.5, and 2.0 cm^3.

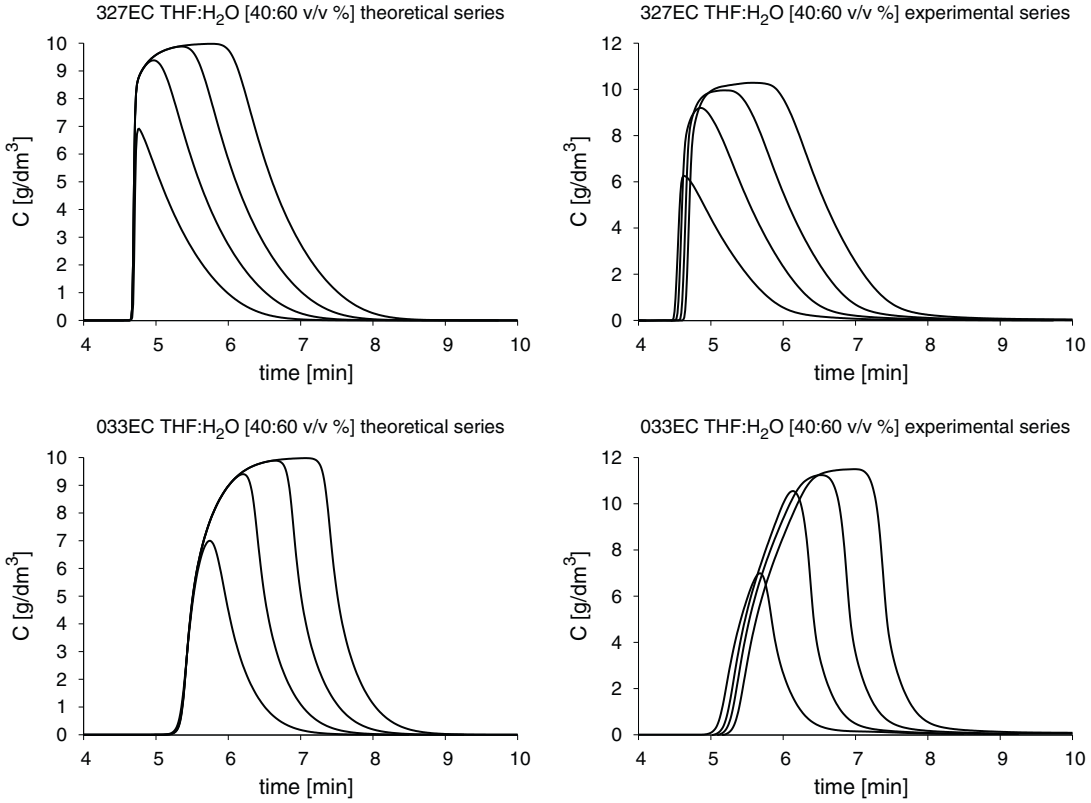

Fig. 9. Same as Fig. 8. except the mobile phase is tetrahydrofuran–water.

between the isotherm parameters derived from FA measurements and from the numerical ED-calculations.

The overloaded elution bands of phenol from acetonitrile–water and tetrahydrofuran–water show a transition from tailing to fronting shape, with the decrease of the surface coverage. During this transition the peak positions not change significantly, this phenomenon can be useful in preparative chromatographic applications.

4.3.4. Effect of the injected amount of phenol on the overloaded bands

To determine the effect of the injected amount of phenol, theoretical and experimental overloaded elution bands were compared. The isotherm parameters derived from the 2.0 cm^3 injections were used to solve the mass-balance equation and simulate the series of overloaded bands with injection volumes of 2.0, 1.5, 1.0 and 0.5 cm^3. The isotherm parameters were unchanged during the calculation process.

The injection of phenol solution results a decrease in the concentration of the organic modifier compared with the equilibrium state of the adsorbent contact with the bulk mobile phase. The parallel positive perturbation with the analyte and the negative perturbation with the organic modifier changes the solvation of the bonded phase during the migration of the band through the column. This affects the shape of the overloaded peaks through the influence on the adsorption properties.

Fig. 8 compares the series of theoretical and experimental overloaded elution bands of phenol on three selected columns from methanol–water mobile phase. The theoretical bands are in good agreement with the experimental ones. The retention time of the fronts decreases with the increase of the injected amount of phenol. The band shapes are constant Langmuir-type overloaded band over the whole range of injected amount of phenol and surface coverage of the columns.

The effect of a stronger eluent (THF) on the overloaded bands can be seen in Fig. 9. With the increase of the injected amount the retention times of the fronts increase, and the deviation from the theoretical series is more pronounced with the decrease of the surface coverage of the C_{18} ligands. The bands shapes, however, remain similar. The increase of the injected amount of phenol solution changes the solvation state of the bonded phase. This results in a change of the peak shape on the same adsorbent, due to the change of the injected amount. Transition from tailing to moderately fronting peak can be observed on columns with medium surface coverage density. The dividing concentration between Langmuir and BET-type overloaded bands decrease with the decrease of the surface coverage. This transition modifies the Langmuir-type adsorption and results in a BET type isotherm. If the concentration of the analyte reaches a border, the retention times of the fronts will increase, and results in a BET-type behavior. This concentration border is represented on the isotherm curve as an inflection point.

5. Conclusions

The chemical modification of the bare silica with alkyl ligands changes not only the polarity of the adsorbent, but the geometry of the pores as well. The change of the average pore radius affects the solvation of the bonded ligands, and the adsorption processes of the analyte molecules. The impact of the pore shape and polarity change can be observed in the solvation and retention processes.

Switching from methanol to a stronger eluent modifies the adsorption behavior of phenol. A transition from monolayer Langmuir to multilayer BET-type adsorption can be observed. The transition is caused by the change in the solvation of the bonded phase, and the enrichment of the organic modifier on the dividing surface between the bulk mobile and the bonded phase. The stronger eluents can effectively block the high-energy adsorption sites, and hamper the partition of phenol to the bonded phase and significantly reduces the saturation capacity of the adsorbent. In parallel, the apolarity of the pores increases and accordingly the equilibrium constant of adsorption of the low energy sites also increases as the increase of hydrophobicity of the organic mobile phase is more pronounced.

The shape of the overloaded elution bands can be modified by changing the organic modifier, or with the change of the carbon load of the adsorbent. The strong effect of the organic modifier on the band shape and on the adsorption isotherm has already been demonstrated in chiral separations [36,37]. The use of strong eluents have the advantage, that the peak shape can be modified from tailing to fronting type without significant shift in the retention time of the phenol band. The disadvantage of the usage of strong eluent is the complication caused by the competition process between the analyte and the solvent molecules, which strengthens as the carbon load of the column decreases. The fronts shift toward lower retention times with the decrease of the injected amount of the analyte. Under those conditions, the competitive pressure of the sample molecules is not enough to reach the high energy sites of the adsorbent. The overloaded elution bands approaches the ideal model with the increase of the injected amount. Finding the optimal organic modifier, as well as the selection of the organic solvent concentration in the aqueous-organic mobile phase is an important tool to maximize the loadability.

Acknowledgements

The work was supported by Ceepus II scholarship CII-PL-0004-03-0708-PL-130-05/06, as well as by Grants OTKA 75717 and OTKA-NKTH 68863. Financial support from European Social Found, Polish National Budget, Kujawsko-pomorskie Voivodship Budget (within Sectoral Operational Programme Human Resources) 'Krok w przyszlosc' and from the Fundation for Polish Science. Professor's Subsidy is gratefully acknowledged. The authors thank Akzo Nobel (Bohus, Sweden) for kind donation of the Kromasil 100 silica gel used in this study. The authors are grateful to Prof. Ferenc Kilár for providing access to the instrumentation funded by Grants GVOP-3.2.1-0168, RET 008/2005.

References

[1] G. Guiochon, A. Felinger, D.G. Shirazi, A. Katti, Fundamentals of Preparative and Nonlinear Chromatography, 2nd ed., Elsevier Academic Press, Amsterdam, 2006.
[2] G. Guiochon, J. Chromatogr. A 965 (2002) 129.
[3] T. Fornstedt, J. Chromatogr. A 1217 (2010) 792.
[4] K. Krupczyska, B. Buszewski, Anal. Chem. 76 (2004) 226.
[5] M. Jaroniec, J. Chromatogr. A 656 (1993) 37.
[6] P. Jandera, M. Skavrada, L. Andel, D. Komers, G. Guiochon, J. Chromatogr. A 908 (2001) 3.
[7] M. Jaroniec, J. Chromatogr. A 722 (1996) 19.
[8] A. Sándi, L. Szepesy, J. Chromatogr. A 845 (1999) 113.
[9] F. Gritti, G. Guiochon, J. Chromatogr. A 1075 (2005) 117.
[10] K.L. Mapihan, J. Vial, A. Jardy, J. Chromatogr. A 1030 (2004) 135.
[11] U.D. Neue, J. Sep. Sci. 30 (2007) 1611.
[12] F. Gritti, G. Guiochon, Anal. Chem. 77 (2005) 4257.
[13] S. Bocian, A. Felinger, B. Buszewski, Chromatographia 68 (2008) 19.
[14] B. Buszewski, S. Bocian, A. Felinger, J. Chromatogr. A 1191 (2008) 72.
[15] F. Gritti, Y. Kazakevich, G. Guiochon, J. Chromatogr. A 1169 (2007) 111.
[16] A. Felinger, G. Guiochon, J. Chromatogr. A 796 (1998) 59.
[17] F. Gritti, G. Guiochon, J. Chromatogr. A 995 (2003) 37.
[18] J. Jacobson, J. Frenz, C. Horváth, J. Chromatogr. 316 (1984) 53.
[19] F. Gritti, G. Gotmar, B.J. Stanley, G. Guiochon, J. Chromatogr. A 988 (2003) 185.
[20] I. Langmuir, J. Am. Chem. Soc. 38 (1916) 2221.
[21] S. Brunauer, P.H. Emmett, E. Teller, J. Am. Chem. Soc. 60 (1938) 309.
[22] E. Morgan, K.W. Burton, G. Nickless, Chemom. Intell. Lab. Syst. 8 (1990) 97.
[23] S. Bocian, P. Vajda, A. Felinger, B. Buszewski, Anal. Chem. 81 (2009) 6334.
[24] B. Buszewski, J. Schmid, K. Albert, E. Bayer, J. Chromatogr. 552 (1991) 415.

[25] B. Buszewski, R.M. Gadzala-Kopciuch, M. Markuszewski, R. Kaliszan, Anal. Chem. 69 (1997) 3277.
[26] J. Samuelsson, P. Sajonz, T. Fornstedt, J. Chromatogr. A 1189 (2008) 19.
[27] L. Pasti, F. Dondi, M. van Hulst, P.J. Schoenmakers, M. Matin, A. Felinger, Chromatographia 57 (2003), S-171.
[28] J. Zhu, A. Katti, G. Guiochon, J. Chromatogr. 552 (1991) 71.
[29] F. Chan, L. Yeung, R. LoBrutto, Y. Kazakevich, J. Chromatogr. A 1082 (2005) 158.
[30] F. Gritti, G. Guiochon, J. Chromatogr. A 1099 (2005) 1.
[31] F. Gritti, G. Guiochon, J. Chromatogr. A 1115 (2006) 142.
[32] J. Samuelsson, L. Edström, P. Forssén, T. Fornstedt, J. Chromatogr. A 1217 (2010) 4306.
[33] F. Gritti, A. Felinger, G. Guiochon, J. Chromatogr. A 1136 (2006) 57.
[34] A. Felinger, F. Gritti, G. Guiochon, J. Chromatogr. A 1024 (2004) 21.
[35] A. Felinger, D. Zhou, G. Guiochon, J. Chromatogr. A 1005 (2003) 35.
[36] R. Arnell, P. Forssén, T. Fornstedt, Anal. Chem. 79 (2007) 5838.
[37] P. Forssén, R. Arnell, T. Fornstedt, J. Chromatogr. A 1216 (2009) 4719.